



Estimation of antenna phase center offset for BDS IGSO and MEO satellites

Guanwen Huang¹ · Xingyuan Yan¹ · Qin Zhang¹ · Chenchen Liu¹ · Le Wang¹ · Zhiwei Qin¹

Received: 19 October 2017 / Accepted: 13 February 2018 / Published online: 24 February 2018
© Springer-Verlag GmbH Germany, part of Springer Nature 2018

Abstract

The BeiDou satellite navigation system (BDS) is different from other global navigation satellite systems (GNSSs) because of its special constellation, which consists of satellites in geostationary earth orbit, inclined geosynchronous earth orbit (IGSO), and medium earth orbit (MEO). Compared to MEO satellites, the observations of IGSO satellites cover only a small range of nadir angles. Therefore, the estimation of phase center offsets (PCOs) suffers from high correlation with other estimation parameters. We have estimated the phase center offsets for BeiDou IGSO and MEO satellites with a direct PCO parameters model, and constraints are applied to cope with the correlation between the PCOs and other parameters. Validation shows that the estimated PCO parameters could be used to improve the accuracy of orbit and clock offset overlaps. Compared with the Multi-GNSS Experiment antenna phase center correction model, the average improvements of the proposed method for along-track, cross-track, and radial components are 19 mm (31%), 5 mm (14%), and 2 mm (15%) for MEO satellites, and 13 mm (17%), 12 mm (21%), and 5 mm (19%) for IGSO satellites. For clock offset overlaps, average improvements of standard deviation and root mean square (RMS) are 0.03 ns (20%) and 0.03 ns (12%), respectively. The RMS of precise coordinates in the BDS-only positioning was also improved significantly with a level of 24 mm (30%) in the up-direction. Finally, the overall uncertainty of the estimated results is discussed.

Keywords BeiDou · Satellite antenna phase center offsets · Improved strategies · Precise orbit determination

Introduction

The BeiDou satellite navigation system (BDS) was developed independently by China. The regional system consists of 14 Beidou-2 satellites with five geostationary earth orbit (GEO) satellites, six inclined geosynchronous earth orbit (IGSO) satellites, and three medium earth orbit (MEO) satellites (Ge et al. 2012; Guo et al. 2016a).

With the rapid development of the constellation of BDS, applications have also shown a gradual trend to high precision. Antenna phase center offsets, which are not only the error source but also translation-parameters of the center of mass, play an important role in precise positioning. On the other hand, inaccurate phase center corrections will also

lead to the uncertainty of the reference frame and degrade the performance of the orbit product. Therefore, the antenna phase center offset must be accurately estimated in-orbit.

The International GNSS Service (IGS) has provided an absolute antenna model with phase center offsets (PCOs) and phase variations (PVs) for both GPS satellites and receivers for more than 10 years. The antenna model applicable for the period of this study (Jan.-Dec. 2015) is igs08.atx. It is consistent with ITRF2008 and also includes a GLONASS antenna model (Schmid et al. 2016). High accurate PCOs for Galileo In-Orbit Validation (IOV) and Full Operational Capability (FOC) satellites were estimated by Steigenberger et al. (2016). For BDS, phase center corrections of IGSO and MEO satellites were estimated by Dilssner et al. (2014) and Guo et al. (2016b). However, there were significant differences between the two estimations of the z -offset for IGSO, and satellites that prevented incorporation of these results into igs08.atx (Montenbruck et al. 2017). Thus, it is necessary to further study the accurate estimation of PCOs for BDS satellites, especially for IGSO satellites.

✉ Xingyuan Yan
yanxydice@163.com

✉ Qin Zhang
zhangqinle@263.net.cn

¹ College of Geology Engineering and Geomatics, Chang'an University, Xi'an 710054, Shanxi, China

For BDS GEO satellites, the static geometry results in an unbalanced distribution of observations on the range of the nadir angle from the ground, and it is difficult to use ground data to estimate the PCOs of GEO satellites. Therefore, this article only focuses on the antenna phase center corrections of IGSO and MEO satellites. This study aims to estimate high-precision PCOs for BDS. First, basic models related to satellites phase center correction are introduced. Then, based on the strategy for estimating PCOs, the daily PCOs corrections are obtained and the corrections time series are analyzed. Final PCOs are derived from the means of daily corrections. Orbit overlaps, clock offset overlaps, and coordinate precision are selected to validate the accuracy of the final PCOs estimations. Furthermore, the performance assessment is compared between the estimated PCOs and the published PCOs and PVs of the European Space Operations Centre (ESOC) and Wuhan University (WHU). A summary of this work is given in the last section.

Basic model

The satellite antenna PCO is a vector directed from the mass center to phase center. It consists of the x -offset, y -offset, and z -offset as three components in a satellite body-fixed coordinate system (Montenbruck et al. 2015a). The PCOs correction model is

$$\vec{r}^{s'} = \vec{r}^s + R \cdot \vec{P} \tag{1}$$

where $\vec{r}^{s'}$ is the vector from receiver antenna phase center to satellite antenna phase center, and \vec{r}^s is the vector from the receiver antenna phase center to the satellite mass center where $\vec{P} = [dx \ dy \ dz]^T$ is the PCOs vector, and dx , dy , and dz are the three components. For convenience, this work used dx , dy and dz in formula derivation, x -offset, y -offset, and z -offset in the text. R is the rotation matrix from body-fixed coordinate to inertial coordinates.

PCO parameters model

The method to estimated PCOs is based on (1), where the PCO parameters are used to transfer from mass center to phase center. Considering the final observation is the distance, the phase center offset correction for a given unit vector $\vec{e}_r = (\sin \alpha \sin \eta, \cos \alpha \sin \eta, \cos \eta)$ of the observation from the satellite to the station can be expressed as

$$\Delta\rho(\alpha, \eta) = -\vec{P} \cdot \vec{e}_r = -dx \cdot \sin \alpha \sin \eta - dy \cdot \cos \alpha \sin \eta - dz \cdot \cos \eta \tag{2}$$

where α is the azimuth and η is the nadir angle seen from the satellite to the station, and the azimuth α is started from the y -axis toward the x -axis of the satellite body-fixed system when viewing from the station. This method estimates PCOs

only in the satellite body-fixed system, directly. However, there are some correlations between the horizontal PCOs (dx and dy) and orbital parameters, between the dz and satellite clock offset, and the correlations between the parameters must be conducted during data processing.

These correlations can be reduced by adding some reasonable constraints. Estimation of the dy component is more stable than others because of the symmetrical satellite structure and the location of the signal transmitter in the y -axis of the IGSO and MEO satellites. Therefore, loose constraints of PCOs were added to the normal equation with 10, 1, and 10 m standard deviation for dx , dy , and dz to improve the stability of the estimation results for the IGSO and MEO satellites. Because the correlation between the dz and satellite clock offset strongly depends on the nadir-angle and this method cannot eliminate the effect of small range of the nadir-angle, we used the mean of the daily dz to get a better final estimation. Therefore, a longer period of about 1 year of data processing is necessary to obtain a more stable estimation of dz , as well as the horizontal PCOs.

Strategies for POD

The Multi-GNSS Experiment (MGEX) is organized by the IGS group in order to track, collect, and analyze all available GNSS signals including GPS, GLONASS, Galileo, BDS, and QZSS. The International GNSS Monitoring and Assessment System (iGMAS) was developed by China independently with its main task to establish a global multi-GNSS tracking network for collecting, processing, and analyzing the data from this network and release precise products for services (Guo et al. 2016b).

The observation data of the iGMAS and MGEX network from January 1 to December 31, 2015, were processed. Figure 1 shows the distribution of the selected stations.

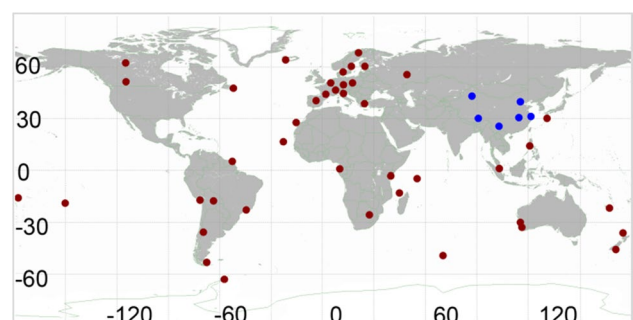


Fig. 1 Distribution of the selected stations. Red cycle stations are from MGEX and blue cycle stations are from iGMAS

Frame scale factor

It is well accepted that the estimation of satellite PCOs can only be obtained by aligning the scale factor to the IGS08 framework (Ge et al. 2005b). Weekly IGS solutions were used as a priori values to constrain the station coordinates. In this work, the scale factor aligned to the IGS08 frame was realized by adding tight constraints to the IGS station coordinate parameters. The PCOs and PVs of GPS satellites were fixed to `igs08_www.atx` files where `www` is the current week number of GPST. Then, the PCOs and PVs of the GPS receiver were also fixed to the robot and field calibrations. However, most of the BDS receivers had no robot calibrations, so L1 and L2 corrections of GPS were used instead of that of B1 and B2 of BDS, respectively.

SRP model

As a widely used solar radiation pressure (SRP) model, the empirical CODE (Center for Orbit Determination in Europe) orbit model (ECOM) was developed by Beutler et al. (1994). This model is expressed in a sun-oriented reference frame, where D points to the Sun, Y goes along with the solar panel axis, and B completes a right-handed system. In each direction, the model comprises a constant term as well as optional sine and cosine terms. A subset of five parameters named ECOM 5 model can be expressed as

$$\begin{aligned} D &= D_0 \\ Y &= Y_0 \\ B &= B_0 + B_c \cdot \cos u + B_s \cdot \sin u \end{aligned} \quad (3)$$

where D_0 , Y_0 , B_0 are three constant parameters; B_c and B_s are cosine and sine terms in B direction, and u is the argument of latitude. The ECOM 5 model has a better performance than other models for BDS IGSO and MEO satellites with a length of 72 h (Lou et al. 2016). Considering BDS has no a priori box-wing model, a loose constraint of $0.1 \mu\text{m/s}^2$ was set for each ECOM-5 model parameter.

Summary of processing

PVs solutions are greatly influenced by the ground station distribution (Fig. 1). PVs and PCOs are strongly correlated and cannot be estimated simultaneously. It is necessary to fix PVs for solving PCOs (Schmid and Rothacher 2003; Schmid et al. 2007). Therefore, we fixed the PVs to zero for estimating the PCO parameters of the BDS IGSO and MEO satellites. Furthermore, the following strategies were applied to improve the accuracy of BDS orbit determination: (1) the combined GPS/BDS, 3 days arc length and the

ECOM 5 parameters model was adopted to improve the orbit determination precision; (2) fixing the ambiguity of the BDS IGSO and MEO satellites to improve the precision of the parameters. The summary of strategies is shown in Table 1.

Estimation of satellite antenna phase center offset

The accuracy of parameter resolution is influenced by the correlation between the parameters. To verify the effect of different constraints on parameter resolution, the data of the day of year (DOY) 203/2015 were selected as a case of high sun elevation above the orbital plane (beta angle) to study the correlations between the PCOs and orbital parameters. The specific correlation coefficient matrix is shown in Fig. 2.

From Fig. 2, there is a strong correlation between the position and velocity parameters of the satellite, and the average of the correlation coefficients reaches 67%, when applying no constraints for the PCOs. The average of correlation coefficients between the y -offset, position, and velocity parameters reaches 79%. The average of the correlation coefficients between the x -offset, and the D_0 , B_c , B_s parameters is 97%. The average of the correlation coefficients between the z -offset, position and velocity parameters is 31%. In contrast, when applying constraints for PCOs, the average of the correlation coefficients between the position and velocity parameters is 56%. The average of the correlation coefficients between the y -offset, position, and velocity parameters is 30%. The correlation between the x -offset and the D_0 , B_c , B_s parameters has no change when compared with that of without constraints. The average of the correlation coefficients between the z -offset, position, and velocity parameters is 7%. In particular, the correlation coefficients between the z -offset and orbital parameters are the smallest.

The C09 results have a similar performance to C06 since these two satellites are located at the same orbital plane. For other satellites, the correlation coefficients also decreased after adding constraints.

PCOs time series

Using the processing strategies of Table 1, we obtained the PCO corrections and their standard deviations for the BDS IGSO and MEO satellites with respect to the initial values of (600, 0, 1100) mm. To ensure the accuracy of the solutions, we artificially removed the satellite results with phase residuals larger than 25 mm during data processing. The horizontal offsets and z -offset corrections are shown in Figs. 3 and 4, respectively.

From Fig. 3, it can be seen that PCO estimations of MEO satellites have a lower scatter than those of the IGSO satellites in general. The reason is that the MEO has a better

Table 1 Strategies for data processing

Items	Description
Number of stations	50 stations
Time interval	From 1 January to 31 December 2015
Observation	Zero-difference GPS/BDS phase and code observations
Sampling rate	300 s
Elevation cut-off angle	3°
Weighting	Elevation-dependent GPS:BDS = 4:1
Ambiguity fixing	MEO and IGSO Adding constraints of double-difference ambiguity fixing to the normal equation (Ge et al. 2005a)
System-bias	A constant value per day for each station
Stations coordinates	Fixed to an IGS week-solution, others from GPS PPP A tight constraint of about 0.1 mm for each component was applied for stations with IGS solutions; for other stations, constraints were set as 10 times of standard deviation (STD)
Orbits	72 h orbital arcs 6 initial positions and velocities Pseudo-stochastic pulses at noon and midnight per satellite
Solar radiation model	ECOM5 (3 constant plus 2 periodic cosine and sine term in B) No a priori model
Earth rotation	Piecewise linear modeling for earth rotation parameters (ERPs)
Ionosphere	The first-order effect eliminated by the ionosphere-free linear combination
Troposphere	A priori tropospheric ZTD computed by Saastamoinen (1973) using the global pressure and temperature model (Boehm et al. 2007); Global Mapping Function (GMF) (Boehm et al. 2006); ZTDs at 2 h interval are estimated as a continuous piecewise linear functions; horizontal gradients estimated with 6 h resolution
Satellites PCOs	GPS: igs08_www.atx BDS: initial values of 600, 0, and 1100 mm for dx , dy , and dz , three constants estimated for each arcs per satellite Constraints are 10, 1, and 10 m for dx , dy , and dz
Satellites PVs	GPS: igs08_www.atx BDS: zero for all satellites
Receiver PCOs and PVs	GPS: igs08_www.atx BDS: using L1 and L2 for B1 and B2

geometry, and the correlations between orbit and PCOs are weaker. For the IGSO satellites, when comparing the scatters of the x -offsets with the sun/orbit angle designated as a beta angle, it is easy to find that larger scatter is always accompanied by larger beta angle, and the scatters of x -offset show a peak-to-peak variation of about 40 cm for C06 and C09, 30 cm for C08, 20 cm for C07 and C10, where the maximum beta angle reaches 77° for C06 and C09, 57° for C08, and 39° for C07 and C10. The peak-to-peak variations of about 20 cm are also found in the y -offset series for the IGSO satellites.

The BDS satellite is a non-cubic body, and the ECOM-5 without a priori box-wing model causes a systematic bias with the beta angle in the x -offsets for such bodies. From the results of C06, C08, and C09 in Fig. 3, it can be seen that the systematic variation of the x -offset is indeed related to the beta angle. Thus, use of an a priori box-wing model for BDS satellites is an optional approach to achieve a more stable x -offset.

It can be seen from Fig. 4 that the scatters of the z -offset correction time series for the MEO satellite (C11, C12, and

C14) and IGSO satellites (C06-C10) are about 0.5 and 2 m, respectively. C07 had a higher scatter than that of other IGSO satellites. In general, the MEO satellites have lower scatters than the IGSO satellites in the z -offset.

Final estimations of PCOs

The estimated PCOs for each satellite are listed in Table 2, as the maximum of the inner-type differences of the x -offset and y -offset are about 4 and 5 cm, there is no significant difference between the same types of satellites. Therefore, the final estimations of the x -offset and y -offset parameters are given by satellite types. However, there are significant differences between the z -offset of each satellite. For the same types of satellites, the maximum of the inner-type difference of MEO z -offset is about 20 cm, and that of IGSO satellites is about 67 cm. The final PCO parameters are shown in Table 3.

For the convenience of comparison with other published PCOs, the estimated PCOs are named CHA. Table 3 lists

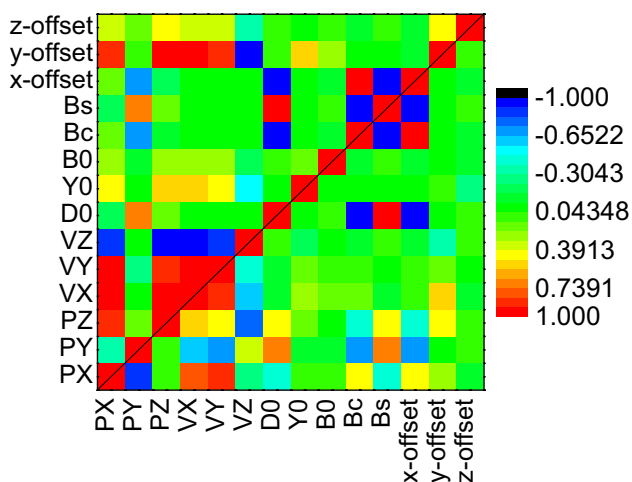


Fig. 2 Correlation coefficients between orbit and PCOs of the C06. *PX*, *PY*, and *PZ* are the position parameters of the satellite, *VX*, *VY*, and *VZ* are velocity parameters, and *D*₀, *Y*₀, *B*₀, *B*_{*c*}, and *B*_{*s*} are the SRP model parameters as defined in (3). The upper triangular part presents the correlation coefficients between the orbital parameters and PCOs without any constraints for PCOs. The lower triangular part shows the correlation coefficients with the constraints for the *x*-offset, *y*-offset and *z*-offset of 10, 1, and 10 m, respectively

the estimations from ESOC (Dilssner et al. 2014) and WHU (Guo et al. 2016b).

From Table 3, it can be seen that: (1) *x*-offset: the deviations of IGSO satellites compared to ESOC and WHU results are -5 and 32 mm, the deviations of the MEO satellites are 23 and -3 mm. (2) *y*-offset: each of organization has the same value 0, no deviation exists; (3) *z*-offset: the

average deviations of IGSO satellites are 74 and 107 cm, and the MEO satellites deviations are 18 and 12 cm. The *x*-offsets of CHA agree well with ESOC and WHU, and the *z*-offset of MEO satellites also has a better consistency with ESOC and WHU; however, the *z*-offset of the IGSO satellites has a poor consistency with a deviation of about 1–2 m.

Validations

To verify the service performance and reliability of the estimated BDS PCOs, we analyzed the accuracy of PCOs from three aspects: orbit overlap, clock offset overlap, and coordinate. Three schemes are set for comparison.

Scheme 1 Precise orbit determination by using the manufacturer’s (MAN) antenna phase center correction model (634, -3 , 1075), named **S1**;

Scheme 2 Precise orbit determination by using MGEX antenna phase center correction model (600, 0, 1100), named **S2**;

Scheme 3 Precise orbit determination by using the CHA model in Table 3 and PVs are zero, named **S3**;

The selected time was from doy 301 to 331 in 2015. Precise orbit determination was implemented according to Schemes 1, 2, and 3, respectively. In addition, coordinates of selected MGEX stations were estimated using the corresponding orbits and clocks results.

Fig. 3 Time series of estimated *x*-offset (black) and *y*-offset (red) correction with respect to the initial values (600, 0, 1100) mm of BDS IGSO/MEO, and the beta angle is blue with the unit of degree, the period of DOY is from 001 to 365 in 2015

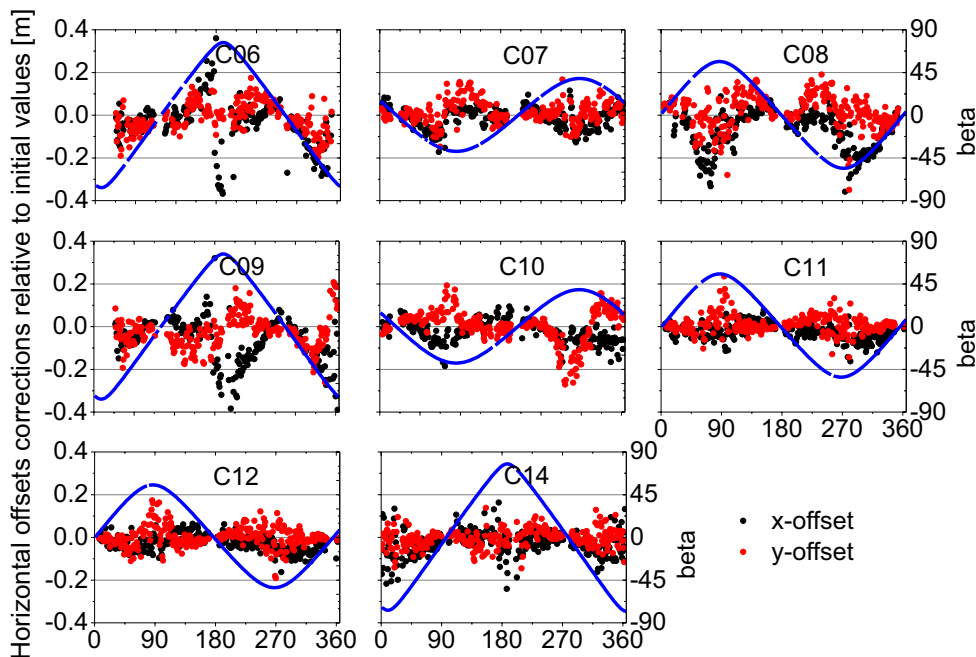


Fig. 4 Time series of the estimated *z*-offset (green) correction with respect to the initial values (600, 0, 1100) mm of BDS IGSO/MEO, the period of DOY is from 001 to 365 in 2015

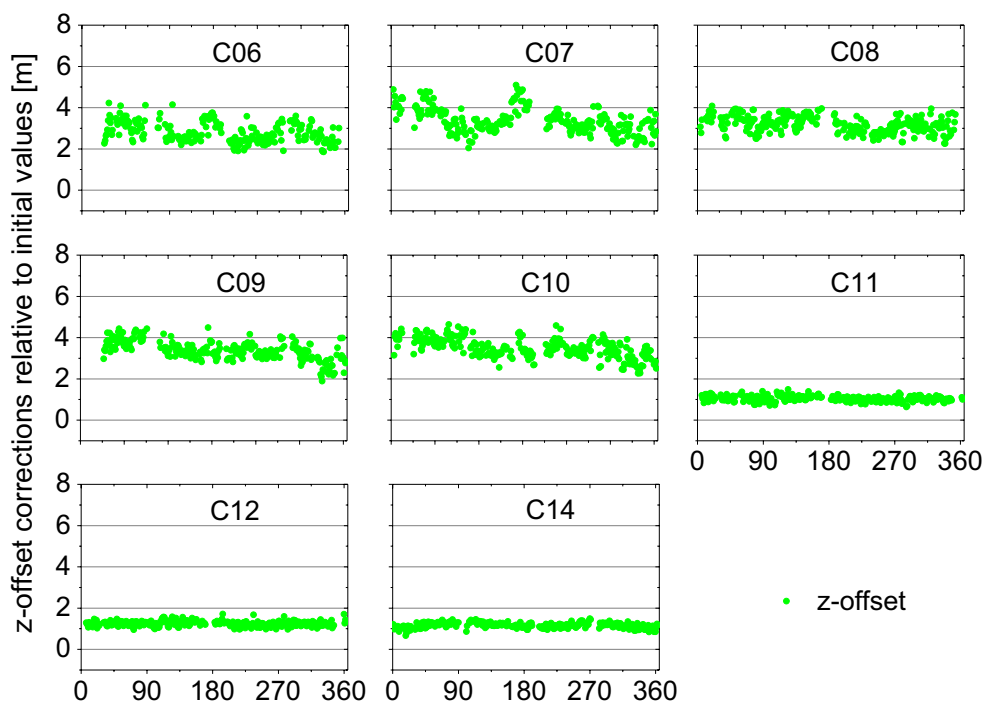


Table 2 Estimated PCOs and STDs for the individual (unit: mm)

PRN	<i>x</i> -offset	<i>y</i> -offset	<i>z</i> -offset	std _{<i>x</i>}	std _{<i>y</i>}	std _{<i>z</i>}
C06	560.56	- 11.17	3894.01	30	50	200
C07	570.92	15.21	4469.97	20	30	210
C08	537.90	18.25	4283.91	20	50	210
C09	530.55	- 27.80	4469.40	30	50	180
C10	570.92	3.94	4571.83	20	30	200
C11	573.94	3.35	2143.34	20	30	70
C12	570.57	1.35	2348.76	20	30	70
C14	571.24	- 3.93	2256.46	20	50	70

Table 3 Estimations of PCOs from CHA, ESOC and WHU (unit: mm)

PRN	CHA			ESOC			WHU		
	<i>x</i> -offset	<i>y</i> -offset	<i>z</i> -offset	<i>x</i> -offset	<i>y</i> -offset	<i>z</i> -offset	<i>x</i> -offset	<i>y</i> -offset	<i>z</i> -offset
C06	554.17	0.00	3894.01	549.00	0.00	3049.00	586.40	0.00	2513.70
C07	554.17	0.00	4469.97	549.00	0.00	3236.70	586.40	0.00	2721.90
C08	554.17	0.00	4283.91	549.00	0.00	3842.60	586.40	0.00	3440.00
C09	554.17	0.00	4469.40	549.00	0.00	3973.60	586.40	0.00	3551.90
C10	554.17	0.00	4571.83	549.00	0.00	3882.10	586.40	0.00	4087.00
C11	572.00	0.00	2143.34	549.00	0.00	2069.50	575.00	0.00	1990.70
C12	572.00	0.00	2348.76	549.00	0.00	2313.50	575.00	0.00	2249.10
C14	572.00	0.00	2256.46	549.00	0.00	2311.70	575.00	0.00	2144.30

Orbit overlap

The RMS of a 24 h orbit overlap is taken as an indicator of validation. Table 4 depicts the average orbit overlap RMS

of the BDS IGSO and MEO in along-track (*A*), cross-track (*C*), and radial (*R*), under the three schemes.

It can be seen from Table 4 that the orbit overlap results of S1 and S2 are at the same level in along-track, cross-track, and radial (*ACR*) directions, the orbit overlap result

Table 4 Different influences between three schemes on orbit overlap accuracy in ACR directions (unit: mm)

PRN	MAN (S1)			MGEX (S2)			CHA (S3)		
	A	C	R	A	C	R	A	C	R
C06	75.23	63.59	24.50	77.45	57.09	24.41	58.41	51.09	19.45
C07	75.77	70.42	26.69	72.92	70.23	27.42	58.65	44.42	20.35
C08	69.17	54.83	26.83	76.03	52.10	25.83	76.21	46.72	22.03
C09	80.00	53.59	25.07	82.00	51.38	24.62	58.31	40.14	20.03
C10	58.86	56.14	20.34	63.03	60.59	19.62	56.59	46.45	16.55
C11	57.31	34.65	16.81	61.88	34.08	14.50	41.31	29.00	12.42
C12	65.00	36.90	16.21	67.00	37.41	14.97	42.41	31.62	12.14
C14	55.93	43.14	15.72	55.50	40.57	15.25	44.21	36.18	13.43
Average of MEO	71.81	59.71	24.69	74.29	58.28	24.38	61.63	45.76	19.68
Average of IGSO	59.41	38.23	16.25	61.46	37.35	14.91	42.65	32.27	12.66

Table 5 Influences between the three schemes on the accuracy of clock offset overlap (unit: ns)

PRN	MAN (S1)			MGEX (S2)			CHA (S3)		
	RMS	STD	Mean	RMS	STD	Mean	RMS	STD	Mean
C06	0.19	0.14	0.13	0.23	0.15	0.17	0.20	0.13	0.16
C07	0.22	0.15	0.17	0.25	0.16	0.19	0.21	0.13	0.17
C08	0.26	0.14	0.22	0.29	0.16	0.24	0.26	0.13	0.23
C09	0.23	0.14	0.18	0.27	0.16	0.22	0.22	0.12	0.19
C10	0.21	0.13	0.17	0.25	0.15	0.20	0.22	0.12	0.18
C11	0.27	0.14	0.23	0.29	0.14	0.25	0.26	0.11	0.24
C12	0.23	0.15	0.17	0.26	0.15	0.22	0.24	0.12	0.21
Average	0.23	0.14	0.18	0.26	0.15	0.21	0.23	0.12	0.19

of S3 has a higher accuracy than that of S1 and S2, except the RMS of C08 has a small increase in the along-track direction. Compared with the S2, average improvements of the S3 for the IGSO satellites are about 13 mm (17%), 12 mm (21%), and 5 mm (19%) in the ACR directions, respectively. The improvements for the MEO satellites are about 19 mm (31%), 5 mm (14%) and 2 mm (15%).

Table 6 Differences between the three schemes on the average RMSs of coordinates in the ENU components (unit: m)

Schemes	E	N	U
MAN(S1)	0.021	0.012	0.083
MGEX (S2)	0.017	0.008	0.080
CHA (S3)	0.014	0.006	0.056

Clock offset overlap

To remove the systematic biases of the 24 h clock offset overlap, the clock offset series were aligned to a reference satellite (Ge et al. 2012). The mean and STD of each satellite clock were used to compute the RMS. Thus, the RMS and STD were selected as the indicators for the clock offset overlap to validate the estimation of the PCOs. The C14 satellite was set as the reference clock. The results of the comparison are shown in Table 5.

Table 6 shows that the CHA PCOs of the S3 improve the STD of the clock offset with the average of 0.12 ns, also have a same level of 0.23 ns with that of S1. Compared with S2, the average STD and RMS of BDS could be improved as much as 0.03 ns (20%) and 0.03 ns (12%), respectively.

Station coordinates

The precise orbit and clock offset products of BDS were used to calculate the precise coordinates of 16 tracking stations (CUT0, DJIG, DYNG, FTNA, GMSD, HARB, JFNG, KIRU, KRGG, KZN2, MAL2, METG, NNOR, NRMG, SIN1, and ZIM3). Reference coordinates were acquired from the IGS solution. The RMSs of biases in east, north and up (ENU) components were selected as the indicators to assess the orbit and clock offset products based on S1, S2, and S3, respectively. The results of the comparison are shown in Table 6.

It can be seen from Table 6 that S1 results in the largest RMSs in ENU directions compared with those of the S2 and S3, and the significant biases in U direction are 8.3 and 8 cm for S1 and S2, respectively. When compared

with that of S2, the RMSs of E direction for most stations of the S3 are significantly improved with an average of 3 mm (17%). For the N-component results, the improvement is 1 mm (16%). For the U-component result, 94% of stations have significant improvement with an average of 24 mm (30%). Therefore, the CHA PCOs could effectively improve the accuracy of the coordinate solution for BDS-only system.

Comparisons with the ESOC and WHU results

For a further comparison with the published PCOs and PVs of BDS, the same indicators were selected to validate the PCOs and PVs released by ESOC (Dilssner et al. 2014) and WHU (Guo et al. 2016b). When the CHA model is adopted, the PVs are set to zero both for the IGSO and MEO satellites.

Orbit and clock offset overlap

The accuracy of orbit overlap and clock offset overlap, obtained from the POD processing by using the PCOs and PVs provided by ESOC, WHU, and CHA was calculated, respectively, and compared with the results by using the MGEX model (S2), which provided the initial values for estimating PCOs. The results of the comparison are shown in Table 7.

It can be seen from Table 7, that when compared with the MGEX model, the overlap accuracy of the IGSO and MEO satellites by using WHU and CHA models all improved. For the average improvements of orbit overlap in each component, the results of the *A* and *R* components of CHA are better than that of WHU and ESOC, and the *C* component of WHU is better than that of CHA and ESOC. For the clock offset overlap, all three PCOs models could improve the accuracy (both RMS and STD). In terms of the average improvements, CHA had the same level of accuracy as WHU, and both the CHA and WHU results are better than that of ESOC.

Table 7 Improvement of the accuracy of orbit and clock offset overlap when compared with the MGEX model

	ESOC (S2–S3)	WHU (S2–S3)	CHA (S2–S3)
Along_track (mm)	– 0.68	10.53	14.97
Cross_track (mm)	5.14	10.26	9.73
Radial (mm)	– 1.83	3.07	3.78
Clk_RMS (ns)	0.02	0.03	0.03
Clk_STD (ns)	0.02	0.03	0.03

Coordinate

After POD processing, we used precise orbit and clock products by using PCOs and PVs provided by ESOC, WHU, and CHA model separately, to estimate the coordinate of BDS-only and compared the accuracy of the coordinate with that of S2. The results of the comparison are shown in Table 8.

It can be seen from Table 8 that the average RMS values of the coordinate using ESOC, WHU, and CHA models are significantly better than that of the MGEX model in the U direction. CHA provides the improvement of 2.4 cm (30%) in the U direction with the same to WHU. In the E direction, the RMS is improved as much as 3 mm (12%) using the CHA model when that of the WHU and ESOC models are 1 mm (6%). In the N direction, the RMS of the CHA model is improved as much as 1 mm (13%), but that of the ESOC and WHU models are degraded by 5 mm (63%).

Conclusions

After analyzing the estimations of the PCOs for BDS, the scatters of the *x*-offset for C06, C08, and C09 exhibited systematic variation are related to the beta angle. The systematic variation might be caused by a non-cubic body (Montenbruck et al. 2015b), and the magnitude of the systematic variation also depends on the maximum of the beta angle, where the larger the maximum beta angle is, the larger the scatter of the *x*-offset series is. Thus, a priori box-wing model for BDS satellites is an available way to enhance the ECOM-5 model and obtain a more stable *x*-offset, especially for IGSO satellites with larger beta angle.

From the validation of PCOs for IGSO and MEO, it was found that the estimations of PCOs could improve the accuracy of orbit and clock offset overlaps as well as BDS PPP. However, from the scatter of IGSO *z*-offset of Fig. 4, it can be concluded that the larger differences of the IGSO *z*-offset are caused by the higher correlation between satellite clock with the smaller range of the nadir-angle of 9° than that of MEO satellites, in this case, the PCO parameters model also suffered from the smaller range of the nadir-angle for IGSO satellites. In addition, the preliminary validation shows that the accuracy of the estimated PCOs of CHA was better than

Table 8 Improvements of the coordinates in the *ENU* components by using ESOC, WHU, and CHA models when compared with the MGEX model (unit: m)

Schemes	<i>E</i>	<i>N</i>	<i>U</i>
ESOC (S2–S3)	0.001	– 0.005	0.023
WHU (S2–S3)	0.001	– 0.005	0.024
CHA (S2–S3)	0.003	0.001	0.024

that of ESOC and WHU. This may be caused by different strategies, updated observations, and procedural consistency. The final performances of different phase center correction models will be validated by the wide users.

Compared the IGSO with MEO, the main difference is the geometry of observations. And the geometries of IGSO and MEO could be quantified by the maximum nadir angle in this work. Figure 4 shows that the larger maximum nadir angles result in a lower correlation of the estimated z -offsets with the clock offsets. Thus, compared with the z -offsets scatters of IGSO and MEO, it was concluded that the scatter of IGSO could be improved by enlarging the maximum nadir angle of observation. On the other hand, for the x -offset and y -offset, the main impact factor is the correlation between the horizontal PCOs and orbit. Compared with the scatters of the PCOs for IGSO and MEO in Fig. 3, if the maximum nadir angle of IGSO could be enlarged, then IGSO has a better geometry of observations, and the impact of the non-cubic body on the systematic variation might be decreased. Adding LEO observations to enlarge the maximum nadir angle can be an alternative approach.

Acknowledgements Thanks for the data support of iGMAS and IGS. This research was partly supported by the National Natural Science Foundation of China (Grant Nos. 41731066, 41774025); the Program of the Grand Projects of the Beidou-2 System (Grant No. GFZX0301040308), the National Natural Science Foundation of Shaan Xi (Grant No. 2016JQ4011), and the Special Fund for Basic Scientific Research of Central Colleges (Grant Nos. 310826172006, 310826172202, 310826173101, Chang'an University). Finally, the authors are also grateful for the comments and remarks of the reviewers, who helped to improve the manuscript significantly.

References

- Beutler G, Brockmann E, Gurtner W, Hugentobler U, Mervart L, Rothacher M, Verdun A (1994) Extended orbit modeling techniques at the CODE processing center of the international GPS service for geodynamics (IGS): theory and initial results. *Manuscr Geod* 19(6):367–386
- Boehm J, Niell A, Tregoning P, Schuh H (2006) Global Mapping Function (GMF): a new empirical mapping function based on numerical weather model data. *Geophys Res Lett* 33(7):L07304. <https://doi.org/10.1029/2005GL025546>
- Boehm J, Heinkelmann R, Schuh H (2007) Short note: a global model of pressure and temperature for geodetic applications. *J Geod* 81(10):679–683. <https://doi.org/10.1007/s00190-007-0135-3>
- Dilssner F, Springer T, Schönemann E, Enderle W (2014) Estimation of satellite Antenna Phase Center corrections for BeiDou. In: *Proceedings of IGS workshop 2014, June 23–27, Pasadena, USA*
- Ge M, Gendt G, Dick G, Zhang FP (2005a) Improving carrier-phase ambiguity resolution in global GPS network solutions. *J Geod* 79(1–3):103–110. <https://doi.org/10.1007/s00190-005-0447-0>
- Ge M, Gendt G, Dick G, Zhang FP, Reigber C (2005b) Impact of GPS satellite antenna offsets on scale changes in global

network solutions. *Geophys Res Lett* 32(6):L06310. <https://doi.org/10.1029/2004GL022224>

- Ge M, Chen J, Dousa J, Gendt G, Wickert J (2012) A computationally efficient approach for estimating high-rate satellite clock corrections in realtime. *GPS Solut* 16:9–17. <https://doi.org/10.1007/s10291-011-0206-z>
- Guo J, Chen G, Zhao Q, Liu J, Liu X (2016a) Comparison of solar radiation pressure models for BDS IGSO and MEO satellites with emphasis on improving orbit quality. *GPS Solut*. <https://doi.org/10.1007/s10291-016-0540-2>
- Guo J, Xu X, Zhao Q, Liu J (2016b) Precise orbit determination for quad-constellation satellites at Wuhan University: strategy, result validation, and comparison. *J Geod* 90(2):143–159. <https://doi.org/10.1007/s00190-015-0862-9>
- Lou Y, Liu Y, Shi C, Wang B, Yao X, Zheng F (2016) Precise orbit determination of BeiDou constellation: method comparison. *GPS Solut* 20(2):259–268
- Montenbruck O, Schmid R, Mercier F, Steigenberger P, Noll C, Fatkulin R, Kogure S, Ganeshan AS (2015a) GNSS satellite geometry and attitude models. *Adv Space Res* 56(6):1015–1029. <https://doi.org/10.1016/j.asr.2015.06.019>
- Montenbruck O, Steigenberger P, Hugentobler U (2015b) Enhanced solar radiation pressure modeling for Galileo satellites. *J Geod* 89(3):283–297. <https://doi.org/10.1007/s00190-014-0774-0>
- Montenbruck O et al (2017) The Multi-GNSS Experiment (MGEX) of the International GNSS Service (IGS)—achievements, prospects and challenges. *Adv Space Res* 59(7):1671–1697. <https://doi.org/10.1016/j.asr.2017.01.011>
- Saastamoinen J (1973) Contributions to the theory of atmospheric refraction, part II: refraction corrections in satellite geodesy. *Bull Geod* 105(1):279–298. <https://doi.org/10.1007/BF02521844>
- Schmid R, Rothacher M (2003) Estimation of elevation-dependent satellite antenna phase center variations of GPS satellites. *J Geod* 77(7–8):440–446
- Schmid R, Steigenberger P, Gendt G, Ge M, Rothacher M (2007) Generation of a consistent absolute phase center correction model for GPS receiver and satellite antennas. *J Geod* 81(12):781–798. <https://doi.org/10.1007/s00190-007-0148-y>
- Schmid R, Dach R, Collilieux X, Jäggi A, Schmitz M, Dilssner F (2016) Absolute IGS antenna phase center model igs08.atx: status and potential improvements. *J Geod* 90(4):343–364. <https://doi.org/10.1007/s00190-015-0876-3>
- Steigenberger P, Fritsche M, Dach R, Schmid R, Montenbruck O, Uhlemann M, Prange L (2016) Estimation of satellite antenna phase center offsets for Galileo. *J Geod* 90(8):773–785. <https://doi.org/10.1007/s00190-016-0909-6>



Guanwen Huang is an associate professor of Chang'an University, Xian, P. R. China. He received a Bachelor, M.Sc., and Ph.D. degrees in Surveying Engineering from Chang'an University, in 2005, 2008, and 2012. His research activities include Precise Point Positioning theory, real-time satellite clock model, and their application.



Xingyuan Yan is a Ph.D. student at the College of Geology Engineering and Geomatics, Chang'an University, Xian, P. R. China. He received his Bachelor degree from Chang'an University in 2014. His research focuses on GNSS precise orbit determination.



Le Wang is a Ph.D. student at the College of Geology Engineering and Geomatics, Chang'an University, Xian, P. R. China. He received his Bachelor degree from Chang'an University in 2012. His research focuses on real-time GNSS precise orbit determination.



Qin Zhang is a professor of Chang'an University, Xian, P. R. China. She received a Bachelor, M.Sc. and Ph.D. degrees in Surveying Engineering from Wuhan University, Wuhan, P. R. China, in 1982, 1994, and 2002. Her current research activities have been mainly related to GNSS and InSAR theory and application.



Zhiwei Qin is a Master graduate student in the College of Geology Engineering and Geomatics, Chang'an University, Xian, P. R. China. He received his Bachelor degree from University of Science and Technology, Liaoning in 2016. His research focuses on GNSS precise orbit determination.



Chenchen Liu is a Ph.D. student at the College of Geology Engineering and Geomatics, Chang'an University, Xian, P. R. China. She received her Bachelor degree from Chang'an University in 2014. Her research focuses on Inertial navigation.